Journal of Fundamental and Applied Sciences

Research Article

ISSN 1112-9867

Available online at http://www.jfas.info

HIGH SENSITIVITY DETECTION OF THE STATOR SHORT-CIRCUIT FAULTS IN INDUCTION MOTOR USING HILBERT PARK'S VECTOR PRODUCT

A. Allal[1,2] and B.Chetate[2]

[1]Department of electrical engineering, Echahid Hamma Lakhdar University of El-Oued, Algeria

[2]Research Laboratory on the Electrification of Industrial Enterprises, University of M'Hamed Bougara of Boumerdes, Algeria

Received: 31 December 2018 / Accepted: 29 April 2019 / Published online: 01 May 2019

ABSTRACT

In this paper, a new approach for induction motor diagnosis, which called: Hilbert Park's Vector Product Approach (HPVPA), is proposed, this processes offers unprecedented a high sensitivity in case of stator faults. In order to highlight the effectiveness of this method, this paper included with an important comparison between the proposed method and the proposed techniques in the recently research works; such as: Motor Square Current Signature Analysis (MSCSA), Park's Vector Square Modulus (PVSM), Park's Vector Product Approach (PVPA), Park-Hilbert "P-H" ($PVSM_{P-H}$) and the classical method: Motor Current Signature Analysis (MCSA). The proposed approach bases on three essential steps: firstly, the Hilbert transform of the three phases currents will be aplicated, and then their instantaneous amplitudes will be extracted. Secondly, their current Park's vector components will be reduced. Finally, we apply the mathematical product of its two current Park's vector components is applicated.

Keywords: Hilbert transform .Induction motor Diagnosis .Inter-turn short- circuit .Park transform Spectral analysis.

Author Correspondence, e-mail: allalabderrahim@yahoo.fr

doi: http://dx.doi.org/10.4314/jfas.v11i2.29

1. INTRODUCTION

Induction motors are commonly used in large range of industrial applications; because of their simple construction, reliability and the availability of power converters using efficient control strategies [1]. It is well known, that detection and diagnosis of faults allow preventive and conditional maintenance of electrical machines during scheduled downtimes and prevent an extended period of breakdown due to wide system failures [2]. For the fault detection problem, it is valuable to know if a fault exists in the system via online measurements [3]. By meaning of the diagnosis, it is not only used to detect the default, but also to locate it and to find its origin [4,5]. A variety of detection methods of induction motor faults are published and proposed by diagnosis research works.

In [6], Sribovornmongkol proposed an on-line induction motor diagnosis system based on the analysis motor current signature analysis (MCSA) with advanced signal processing algorithms is proposed by [7].

In recent years; we have found in [8-10], authors who propose a more advanced signal processing method based on Park-Hilbert Transform “Park-Hilbert” ($PVSM_{P-H}$) [11] used the line current to obtain “motor square current signature analysis” (MSCSA) and “Park’s Vector Square Modulus” (PVSM) have also used by [8-10,12] .

In this work, an original technique will be proposed, which is called “Hilbert Park’s Vector Product” Approach (HPVPA). This new method is inspired from [7-12]) and especially our last paper [13,14] where we have used “ Park’s Vector Product Approach (PVPA) for Induction Motors Diagnosis” which is based on an improved combination of Hilbert and Park transforms. Starting from this combination, we can release two fault signatures: Hilbert direct current Park (I_{dP-H}) and Hilbert reverse current Park (I_{qP-H}). The product of these two signatures HPVPA is subsequently analyzed using the classical fast Fourier transform (FFT).
We will compare our new technique HPVPA to approaches proposed in the paper recently published. We also aim at identifying the efficiency, the sensitivity, the advantages and strong points of our new proposed diagnostic method.

2. Stator Current Harmonics in Induction Motor

The air gap field of an induction motor fed by a sinusoidal voltage supply waveform comprises a wide range of different space harmonics [15]. The following analysis assumes that these air-gap flux harmonics are a result of the interaction of air-gap permeance with harmonic magnetomotive force (MMF) waves [16, 17]. Knowing that only harmonics due to slotting are considered here (rotor slot harmonics). In [15,16], rotor slots harmonics (RSH) generated in the stator line current are presented for a healthy machine at frequencies given by Eq. (1) :

$$f_{RSH}(k,s)=\left|\left(1\pm\frac{kN_r}{p}(1-s)\right)f_s\right|_{k=1,2,3,...} \tag{1}$$

Where , k :is a positive integer, "1" is a fundamental harmonic , s : is the slip , N_r : is the number of rotor slot, p : is the number of pole pairs, f_s : is the fundamental supply frequency .

For a stator winding formed of three identical coils and fed by a balanced voltage system, one must find, only the currents (induced by induction), the rank is odd, and is not a multiple of three. Therefore, we note that only the RSH who's their order belongs to the following set can be detected [15] :

$$G=\left\{\left(\left(\frac{kN_r}{p}\pm 1\right)_{k=1,2,3,..}\right)\cap(6\nu\pm 1)_{\nu=1,2,3,..}\right\} \tag{2}$$

ν : is a positive integer

For against, and in practice there is always a certain level stator unbalance from different origins (problems in the supply voltage or residual asymmetry in stator windings or neutral connection); in this case, all the harmonics, even those having a multiple rank of three will be present in the spectrum of the stator current. Finally, we can see that for a healthy functioning, the stator current of an induction motor cage consists of two series of harmonics [8-10,18] :

1-A series of harmonics of the time (TH) of frequency:

$$f_{TH}(h)=hf_s \quad \text{or} \quad TH=hf_s \tag{3}$$

2-A series of harmonics of rotor slots (RSH) of frequency:

$$f_{RSH}(h,k,s)=\left|\left(h\pm\frac{kN_r}{p}(1-s)\right)f_s\right| \quad \text{or} \quad S^{\pm}=\left|(h\,f_s\pm kN_r\,f_r)\right| \tag{4}$$

Where, $h=1,3,5,\ldots$ is the time harmonic order.

And in practice, we also have other harmonics called Rotor Bar Fault Harmonics (RBFH), due to the inherent rotor cage asymmetries. On the other hand, we notice the Eccentricity Fault Harmonics (EFH) due to the inherent level of mixed eccentricity. We can see that for a healthy functioning, stator current of an induction motor cage consists of two other following series of harmonics given by [8-10,18,19] :

3- A series of Harmonics of Rotor Bar Fault ((RBFH) of frequency

$$f_{RBFH}(h,k,s)=\left|(h\pm 2ks)f_s\right| \quad \text{or} \quad R^{\pm}=\left|(h\pm 2ks)f_s\right| \tag{5}$$

4- A series of harmonics of Eccentricity Fault (EFH) of frequency:

$$f_{EFH}(h,k,s)=\left|(h\pm\frac{kN_r}{p}(1-s))\,f_s\right| \quad \text{or} \quad E^{\pm}=\left|(hf_s\pm kN_r\,f_r)\right| \tag{6}$$

Where: $f_r=\left(\frac{N_r}{p}(1-s)\,f_s\right)$: is the mechanical rotor speed. (See Table 1).

3. Study of the Stator Current with its Harmonics

We will focus our study around the phase currents .Because our work and mathematical calculations are based essentially on fundamental and all existing harmonics. Thus, the instantaneous current circulating in the phase "a","b" and "c", of our three-phase asynchronous motor [8,20] is given by (Eq.7):

$$\begin{cases} i_{sa}(t)_{\text{healthy}}=\hat{I}_F\cos(2\pi f_s t) \\ i_{sb}(t)_{\text{healthy}}=\hat{I}_F\cos\left(2\pi f_s t-\frac{2\pi}{3}\right) \\ i_{sc}(t)_{\text{healthy}}=\hat{I}_F\cos\left(2\pi f_s t-\frac{4\pi}{3}\right) \end{cases} \tag{7}$$

And we will replace the harmonics mentioned above in the expressions given by [8,20].These

equations become as follows Eq.(8):

where $\hat{I}_{THh}$, $\hat{I}_{S^{\pm}k}$, $\hat{I}_{R^{\pm}k}$ and $\hat{I}_{E^{\pm}k}$ are , respectively, the supply phase maximum current for the TH , RSH, RBFH and EFH (amperes)(see Table 1 and Fig.3.); and, finally, t : is the real time (seconds). With, $m = 1,3,5,7,9,...$ and $n = 1,2,3,4,...$

Table 1. General expression of the different harmonics of the stator current [8-10, 18]

Harmonic Types	***The general expression of their frequencies in Current Spectrum:***	***Their causes***
Time Harmonics (TH):	$TH = hf_s$	Imposed by the supply source or residual asymmetry in stator windings
Rotor Slot Harmonics (RSH)	$S^{\pm} = \left\|(h f_s \pm N_r f_r)\right\|$	Imposed by the rotor structure (discrete distribution of the rotor bars in rotor slots)
Rotor Bar Fault Harmonics (RBFH)	$R^{\pm} = \left\|\left(h \pm 2ks\right) f_s\right\|$	Due to the inherent rotor cage asymmetries
Eccentricity Fault Harmonics (EFH)	$E^{\pm} = \left\|(hf_s \pm kf_r)\right\|$	Due to the inherent level of mixed eccentricity

$$\begin{cases} i_{sa}(t)_{\text{healthy}} = \sum_{h=1}^{m}\left[\hat{I}_{THh}\cos\left(2\pi TH\ t\right) + \sum_{k=1}^{n}\left[\hat{I}_{S^{\pm}h}\cos\left(2\pi S^{\pm}\ t\right) + \hat{I}_{R^{\pm}k}\cos\left(2\pi R^{\pm}t\right)\right.\right. \\ \qquad \left.\left. + \hat{I}_{E^{\pm}k}\cos\left(2\pi E^{\pm}t\right)\right]\right] \\ i_{sb}(t)_{\text{healthy}} = \sum_{h=1}^{m}\left[\hat{I}_{THh}\cos\left(2\pi TH\ t - \frac{2\pi}{3}\right) + \sum_{k=1}^{n}\left[\hat{I}_{S^{\pm}h}\cos\left(2\pi S^{\pm}\ t - \frac{2\pi}{3}\right)\right.\right. \\ \qquad \left.\left. + \hat{I}_{R^{\pm}k}\cos\left(2\pi R^{\pm}t - \frac{2\pi}{3}\right) + \hat{I}_{E^{\pm}k}\cos\left(2\pi E^{\pm}t - \frac{2\pi}{3}\right)\right]\right] \\ i_{sc}(t)_{\text{healthy}} = \sum_{h=1}^{m}\left[\hat{I}_{THh}\cos\left(2\pi TH\ t - \frac{4\pi}{3}\right) + \sum_{k=1}^{n}\left[\hat{I}_{S^{\pm}h}\cos\left(2\pi S^{\pm}\ t - \frac{4\pi}{3}\right)\right.\right. \\ \qquad \left.\left. + \hat{I}_{R^{\pm}k}\cos\left(2\pi R^{\pm}t - \frac{4\pi}{3}\right) + \hat{I}_{E^{\pm}k}\cos\left(2\pi E^{\pm}t - \frac{4\pi}{3}\right)\right]\right] \end{cases} \quad (8)$$

Park transformation is used to transform stator currents from the three-phase system (A-B-C) to the two-phase system (D-Q). The expression for transformation is as presented by [6, 21-23]:

$$i_{sd}(t) = (\frac{\sqrt{2}}{\sqrt{3}})i_{sa}(t) - (\frac{1}{\sqrt{6}})i_{sb}(t) - (\frac{1}{\sqrt{6}})i_{sc}(t) \quad (9)$$

$$i_{sq}(t) = (\frac{1}{\sqrt{2}})i_{sb}(t) - (\frac{1}{\sqrt{2}})i_{sc}(t) \quad (10)$$

In an ideal condition, when only fundamental harmonics exist, the $i_{sq}(t)$ and $i_{sd}(t)$ in Eqs (9) and (10) have physical meanings, and are simplified in steady state such as [24]:

$$i_{sd}(t)_{\text{healthy}} = \frac{\sqrt{6}}{2}\hat{I}_{TH1}\sin(2\pi f_s\ t) \quad (11)$$

$$i_{sq}(t)_{\text{healthy}} = \frac{\sqrt{6}}{2}\hat{I}_{TH1}\cos(2\pi f_s\ t) \quad (12)$$

But , under abnormal conditions, with the unwanted harmonics such as odd harmonics in stator current due to asymmetry in motor structure and/or power supply [6,24] ,and after the replacement in their equations, we find the following expressions:

$$i_{sd}(t)_{\text{healthy}} = \frac{\sqrt{6}}{2}\left[\sum_{h=1}^{m}\left[\hat{I}_{THh}\sin(2\pi TH\ t) + \sum_{k=1}^{n}\left[\hat{I}_{S^{\pm}h}\sin(2\pi S^{\pm}\ t) + \hat{I}_{R^{\pm}k}\sin(2\pi R^{\pm}t)\right.\right.\right.$$
$$\left.\left.\left. + \hat{I}_{E^{\pm}k}\sin(2\pi E^{\pm}t)\right]\right]\right] \quad (13)$$

$$i_{sq}(t)_{\text{healthy}} = \frac{\sqrt{6}}{2}\left[\sum_{h=1}^{m}\left[\hat{I}_{THh}\cos(2\pi TH\ t) + \sum_{k=1}^{n}\left[\hat{I}_{S^{\pm}h}\cos(2\pi S^{\pm}\ t) + \hat{I}_{R^{\pm}k}\cos(2\pi R^{\pm}t)\right.\right.\right.$$
$$\left.\left.\left. + \hat{I}_{E^{\pm}k}\cos(2\pi E^{\pm}t)\right]\right]\right] \quad (14)$$

4. Detection of inter-turn short-circuit in the stator winding fault

When a short circuit happens, phase windings have less numbers of turns, so consequently they will produce less MMF. Furthermore, the currents that flow in the shorted windings will also produce MMF, which is opposite to the main MMF produced by the phase windings [6].This deformation of the netting air-gap MMF, will certainly generates harmonics in the

stator current with characteristic frequencies components [6,25], so the following notes can be extracted:

a)- All TH raise significantly due to inter-turn short-circuit.

b)- This fault increased considerably the majority of the RSH

c)- The amplitudes of RBFH, which represent the theoretical signatures of broken rotor bars, are also increased notably due to the inter-turn short circuit.

d)- All the amplitudes of EFH which represent the theoretical signatures of the air-gap eccentricity, are also strongly augmented [8-10,12] (show Figure 3).

In this study, the very small increase in slip during the default will be ignored : $(s' \approx s)$. Thus, the expression of the stator current during an inter-turn short-circuits in the stator-winding fault is:

$$i_{sa}(t)_{\text{Faulty}} = \sum_{h=1}^{m}\left[\hat{I}'_{THh}\cos(2\pi TH\ t) + \sum_{k=1}^{n}\left[\hat{I}'_{S^{\pm}h}\cos(2\pi S^{\pm}\ t) + \hat{I}'_{R^{\pm}k}\cos(2\pi R^{\pm}t) + \hat{I}'_{E^{\pm}k}\cos(2\pi E^{\pm}t)\right]\right] \quad (15)$$

With: $\hat{I}'_{THh} \neq \hat{I}_{THh}$, $\hat{I}'_{S^{\pm}h} \neq \hat{I}_{S^{\pm}h}$, $\hat{I}'_{R^{\pm}k} \neq \hat{I}_{R^{\pm}k}$ and $\hat{I}'_{E^{\pm}k} \neq \hat{I}_{E^{\pm}k}$ (s' :is the slip of a faulty state)

5. Theory of the Hilbert transform

The Hilbert transform is a linear operator which takes a signal $s(t)$ and produces a transform H(t) in the same domain. The operator can be considered as a time domain convolution defined by the following equation [14, 26]:

$$\widetilde{S}(t) = \frac{1}{\pi}\int_{-\infty}^{+\infty}\frac{S(\tau)}{t-\tau}\,d\tau \quad (16)$$

The complex form of the signal is known as analytic signal. The unique complex representation of a real signal $s(t)$ is given by [27]:

$$\widetilde{S}(t) = \widetilde{S}(t)_{\text{Re}} + j\widetilde{S}(t)_{\text{Im}} \quad (17)$$

Using the mean value theorem, we can evaluate [27]:

$$\widetilde{S}(t)=\frac{1}{\pi\ t}\otimes S(t) \tag{18}$$

Therefore, Hilbert transform is obtained if the original signal, $s(t)$, is convolved with $\frac{1}{\pi\ t}$, if the signal is of the form, $a(t).\cos\Phi(t)$ Which is like a real signal and may be written as [27] :

$$\widetilde{S}(t)=\widetilde{S}(t)_{\mathrm{Re}}+j\widetilde{S}(t)_{\mathrm{Im}}=a(t)\cos\Phi(t)+jH[a(t)\cos\Phi(t)] \tag{19}$$

$$\text{Or}\quad ,\quad \widetilde{S}(t)=a(t)[\cos\Phi(t)+j\sin\Phi(t)] \tag{20}$$

$$\text{Or}\ ,\quad \widetilde{S}(t)=a(t)e^{j\Phi(t)} \tag{21}$$

The Hilbert transform produces a complex time series. The envelope, which is the magnitude of this complex time series, is a representation of the estimate of the modulation contained in the signal due to lateral bands (the instantaneous amplitude $a(t)$), as defined by next equation [7,26] :

$$a(t)=\sqrt{\widetilde{S}(t)_{\mathrm{Re}}{}^{2}+\widetilde{S}(t)_{\mathrm{Im}}{}^{2}} \tag{22}$$

The function of phase modulation (instantaneous phase) $\Phi(t)$ is expressed as [7]:

$$\Phi(t)=\arctan\frac{\widetilde{S}(t)_{\mathrm{Im}}}{\widetilde{S}(t)_{\mathrm{Re}}} \tag{23}$$

6. Detection Fault Using Hilbert Park's Vector Product Approach (HPVPA)

Mathematically, the Hilbert Park's Vector Product Approach (HPVPA) is defined by the previous equations (16)-(23).

The Hilbert transform of a stator current, which is called the analytical signal, is given by the following expression [8-10]:

$$i_{sa}(t)\overset{T}{\Rightarrow}\overset{H}{\Rightarrow}\widetilde{i}_{sa}(t)=\widetilde{i}_{\mathrm{Re}}(t)+j\widetilde{i}_{\mathrm{Im}}(t) \tag{24}$$

The instantaneous amplitude according to the equation (22), of a stator current is obtained by the below equation [8-10]:

$$\left|\widetilde{i}_{sa}(t)\right|=\sqrt{\widetilde{i}_{\mathrm{Re}}(t)^{2}+j\widetilde{i}_{\mathrm{Im}}(t)^{2}} \tag{25}$$

So this approach is mainly constructed on the following stages:

1) Determination of the instantaneous amplitude for each stator currents : $\left|\tilde{i}_{sa}(t)\right|$, $\left|\tilde{i}_{sb}(t)\right|$ and $\left|\tilde{i}_{sc}(t)\right|$.

2) Calculation of the following components : i_{dP-H} and i_{qP-H}

$$\begin{aligned} i_{dP-H} &= (\frac{\sqrt{2}}{\sqrt{3}})\left|\tilde{i}_{sa}(t)\right| - (\frac{1}{\sqrt{6}})\left|\tilde{i}_{sb}(t)\right| - (\frac{1}{\sqrt{6}})\left|\tilde{i}_{sc}(t)\right| \\ i_{qP-H} &= (\frac{1}{\sqrt{2}})\left|\tilde{i}_{sb}(t)\right| - (\frac{1}{\sqrt{2}})\left|\tilde{i}_{sc}(t)\right| \end{aligned} \tag{26}$$

3) Finally, the Hilbert Park's Vector Product Approach (HPVPA) is obtained by the following FFT expression analysis (Show Fig.1. and Fig.8):

$$\text{HPVPA} = i_{dP-H} \times i_{qP-H} \tag{27}$$

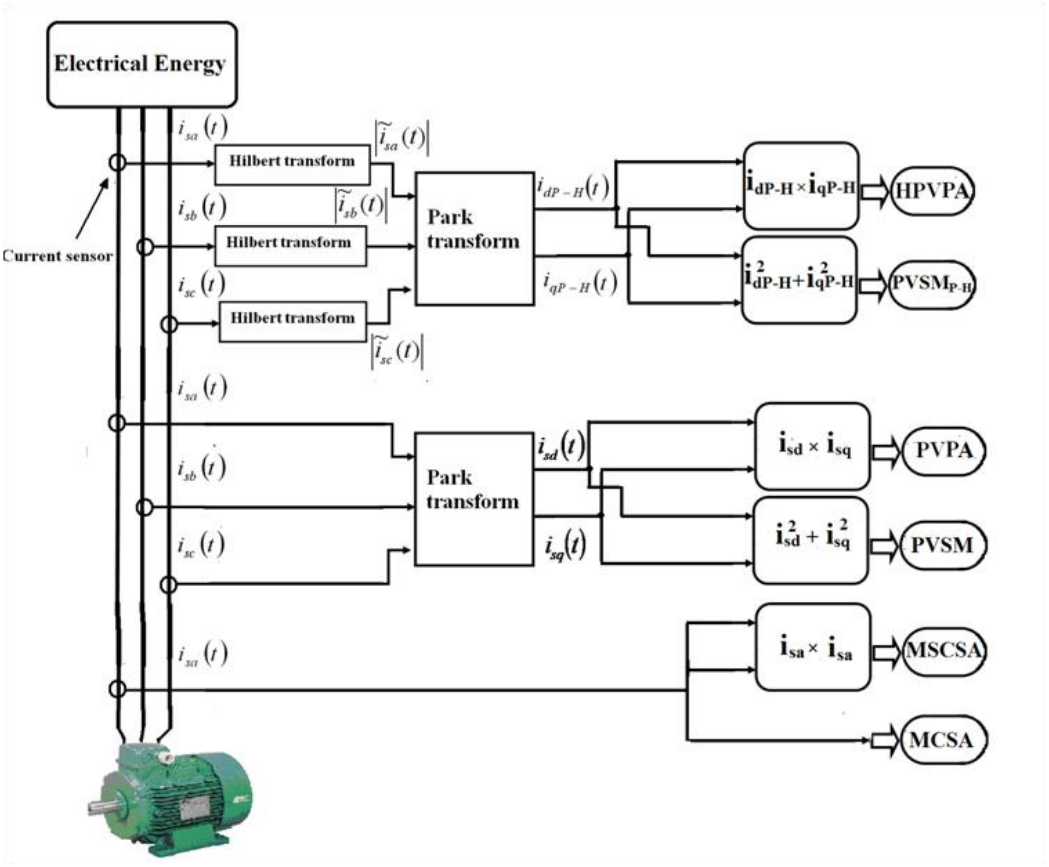

Fig.1. Stator Faults diagnosis in induction motor with the use of different approaches

7. The most used diagnosis fault approaches

7.1. Motor square current signature analysis (MSCSA)

MCSA approach uses the spectrum analysis of one motor stator phase current. The proposed approach is based mainly on the spectrum analysis of the square stator phase current. In this proposed approach MSCSA, for a healthy motor the spectrum of the square current has a fundamental component at the frequency $2f_s = (2\omega_s)/(2\pi)$ along with a DC component, as presented in the figure 1 and figure 5 [11]:

$$\text{MSCSA} = i_{sa}{}^2(t) \tag{28}$$

The analytical computation is simplified and only the harmonics whose amplitude is important will be taking in consideration. So, the harmonics: $\hat{I}_{R^{\pm}k}.\hat{I}_{E^{\pm}k}$, $\hat{I}_{R^{\pm}k}.\hat{I}_{S^{\pm}k}$, and $\hat{I}_{S^{\pm}k}.\hat{I}_{E^{\pm}k}$ will be neglected.

Therefore, we compute successively and separately the following expressions:

$$\begin{aligned} &\text{a)}\ \ h=1,\ TH=f_s\ ,\ k=1 \quad R^{\pm}=(1\pm 2s)\ f_s\,. \\ &\text{b)}\ \ h=1,\ TH=f_s\ ,\ k=1 \quad S^{\pm}=\left|f_s \pm N_r f_r\right|. \\ &\text{c)}\ \ h=1,\ TH=f_s\ ,\ k=1 \quad E^{\pm}=\left|f_s \pm k f_r\right|. \end{aligned} \tag{29}$$

$$i_{sa}(t)_{healthy} = \hat{I}_{TH1}\cos(2\pi f_s t) + \hat{I}_{R^-k}\cos(2\pi(1-2s)\ f_s t) + \hat{I}_{R^+k}\cos(2\pi(1+2s)\ f_s t) \tag{30}$$

The instantaneous square phase current is given by [11] and after replacement in his equation, we find our following expression:

$$\begin{aligned} \text{MSCSA} = i_{sa}{}^2(t)_{healthy} &= \left(\frac{\hat{I}^2{}_{TH1}}{2} + \frac{\hat{I}^2{}_{R^-k}}{2} + \frac{\hat{I}^2{}_{R^+k}}{2}\right) \\ &+ \left(\frac{\hat{I}^2{}_{TH1}}{2} + \hat{I}_{R^-k}\hat{I}_{R^+k}\right)\cos(2\pi(2f_s)\ t) + \left(\hat{I}_{TH1}\hat{I}_{R^-k} + \hat{I}_{TH1}\hat{I}_{R^+k}\right)\cos(2\pi s(2f_s)\ t) \\ &+ \hat{I}_{R^-k}\hat{I}_{R^+k}\cos(2\pi s(4f_s)\ t) + \hat{I}_{TH1}\hat{I}_{R^-k}\cos(2\pi(1-s)(2f_s)\ t) \\ &+ \hat{I}_{TH1}\hat{I}_{R^+k}\cos(2\pi(1+s)(2f_s)\ t) + \frac{\hat{I}^2{}_{R^-k}}{2}\cos(2\pi(1-2s)(2f_s)\ t) \\ &+ \frac{\hat{I}^2{}_{R^+k}}{2}\cos(2\pi(1+2s)(2f_s)\ t) \end{aligned} \tag{31}$$

Equation 31 shows a DC component, $2f_s$ frequency component, and harmonic components at

frequencies $(1\pm ks)2f_s, (1\pm 2ks)2f_s$ .The spectrum of this square current, presented which presented in figure 5, contains additional components at frequencies $2skf_s$ [11,28] .

The expressions in a general way can be written as following:

$$h=1\rightarrow \begin{cases} 0\text{ Hz , is the DC component.} \\ 2f_s \end{cases}$$ Thus we can make a general formula: $TH=(h\pm 1)f_s$. (32)

With h is a pair number $h=1,3,5,7,\ldots$ it is more practical to take $TH=(h-1)f_s$

$$h=1\rightarrow \begin{cases} 2sf_s. \\ 4sf_s \end{cases}$$ the deduced general formula is: $((h-1)\pm 2ks)f_s$ (33)

$$h=1\rightarrow \begin{cases} (1-s)2f_s \\ (1+s)2f \end{cases}$$ the deduced general formula is: $(h\pm ks)2f_s$ (34)

$$h=1\rightarrow \begin{cases} (1-2s)2f_s \\ (1+2s)2f_s \end{cases}$$ the deduced general formula is: $(h\pm 2ks)2f_s$ (35)

Therefore, we can draw that:

$TH=(h-1)f_s$

$R^{\pm}=\left|((h-1)\pm 2ks)f_s\right|$, $R^{\pm}{}'=\left|(h\pm ks)f_s\right|$ and $R^{\pm}{}''=\left|(h\pm 2ks)f_s\right|$

The amplitude of $R^{\pm}$ is more great then $R^{\pm'}$ and $R^{\pm''}$ because $\hat{I}_{TH1}\rangle\rangle \hat{I}^2{}_{R^+k}/2$ and $\hat{I}_{TH1}\rangle\rangle \hat{I}_{TH1}\hat{I}_{R^+k}$

In current comparison, study case, only: $R^{\pm}=\left|((h-1)\pm 2ks)f_s\right|$ is taken

As the same previous procedure, for the other harmonics, calculation is included:

$$TH=(h-1)f_s \text{ and } R^{\pm}=\left|((h-1)\pm 2ks)f_s\right|$$

$$S^{\pm}=\left|((h-1)f_s\pm N_r(1-s))f_s\right|$$

$$E^{\pm}=\left|((h-1)f_s\pm k(1-s))f_s\right| \quad (36)$$

The same computations for b) and c) of equation 29.

It is noted that, our proposed approach HPVPA ,PVSM , PVPA and $PVSM_{P-H}$ has the same harmonics as those of MSCSA cited, above. Without simplification of the computation, we find all the different harmonics in Table 2.

Note: We will find the same expressions in the case where there would be a default, but we replace only $\hat{I}$ by $\hat{I}'$, with $\hat{I} \neq \hat{I}'$ and the same procedure for the following operations.

7.2. Park's vector square modulus (PVSM)

Recently used and giving good results method for detection of faults in electrical machines is analyzing the spectrum of Park's Vector absolute value [29].

Considering TH and $R^{\pm}$ harmonics only and taking into account the Eqs. (13) and (14), it can be shown that Park's vector square modulus will be equal to the equation given by [24] and we will replace it in the equation given by [24].This equation become as follows:

$$\left|i_{sd} + j\ i_{sq}\right|^2 = \frac{3}{2}(\hat{I}^2{}_{TH1} + \hat{I}^2{}_{R^-k} + \hat{I}^2{}_{R^+k}) + 3\hat{I}_{TH1}\hat{I}_{R^-k}\cos(2\pi s(2f_s)\ t)$$
$$+3\hat{I}_{TH1}\hat{I}_{R^+k}\cos(2\pi s(2f_s)\ t) + 3\hat{I}_{R^-k}\hat{I}_{R^+k}\cos(2\pi s(4f_s)\ t) \quad (37)$$

Consequently, in the Eq.(37) the Park's Vector Square Modulus spectrum is the sum of a DC level, generated mainly from the fundamental component of power supply, plus two additional terms at frequencies $2sf_s$ and $4sf_s$ .In general $2ksf_s$,(See Fig.1. and Fig.4 .)[24]:

The expressions can be deduced in a general way:

$h = 1 \rightarrow \{0$ Hz is the DC component. Thus, we can make a general formula: $TH = (h-1)f_s$

$$h = 1 \rightarrow \begin{cases} 2sf_s \cdot \\ 4sf_s \end{cases}$$ we can deduce a general formula $((h-1) \pm 2ks)f_s$ (38)

Therefore, we can draw that:

$$TH = (h-1)f_s$$
$$R^{\pm} = \left|((h-1) \pm 2ks)f_s\right| \quad (39)$$

It is noted that, the approach $PVSM_{P-H}$ studied below , has the same harmonics as those of

PVSM cited, above, Table 2.

7.3. Park–Hilbert Method ($PVSM_{P-H}$)

Mathematically, the Park–Hilbert method is defined by Eqs. (24) - (26) and used by [8-10] but the Eq. (27) is changed by the following expression (See Fig.1. and Fig.6):

$$\mathrm{PVSM}_{\mathrm{P\text{-}H}} = \left(\sqrt{i^2{}_{dP-H} + i^2{}_{qP-H}}\right)^2 \tag{40}$$

7.4. Park's Vector Product Approach (PVPA)

Our last paper [13, 14] where we have used " Park's Vector Product Approach (PVPA) for Induction Motors Diagnosis" is mainly based on the product of $\boldsymbol{i_d}$ with $\boldsymbol{i_q}$ current (See Fig.1):

$$\mathrm{PVPA} = i_{sd}(t)\ .\ i_{sq}(t) \tag{41}$$

We will simplify the analytical computation and we will taking into consideration only Eccentricity Fault Harmonics with:

$$i_{sd}(t)_{\mathrm{healthy}} = \frac{\sqrt{6}}{2}\left(\hat{I}_{TH1}\sin(2\pi f_s\ t) + \hat{I}_{E^{-}1}\sin(2\pi(f_s - f_r)t) + \hat{I}_{E^{+}1}\sin(2\pi(f_s + f_r)t)\right) \tag{42}$$

$$i_{sq}(t)_{\mathrm{healthy}} = \frac{\sqrt{6}}{2}\left(\hat{I}_{TH1}\cos(2\pi f_s\ t) + \hat{I}_{E^{-}1}\cos(2\pi(f_s - f_r)t) + \hat{I}_{E^{+}1}\cos(2\pi(f_s + f_r)t)\right) \tag{43}$$

In this situation, the PVPA is given by:

$$\begin{aligned} i_{sd}(t)\ .\ i_{sq}(t) = {} & \frac{3}{4}\hat{I}^2{}_{TH1}\sin(2\pi(2f_s)\ t) + \frac{3}{4}\hat{I}^2{}_{E^{-}1}\sin(2\pi(2(f_s - f_r))t) \\ & + \frac{3}{4}\hat{I}^2{}_{E^{+}1}\sin(2\pi(2(f_s + f_r))t) - \frac{3}{2}\hat{I}_{TH1}\hat{I}_{E^{-}1}\sin(2\pi(2f_s - f_r)t) \\ & + \frac{3}{2}\hat{I}_{TH1}\hat{I}_{E^{+}1}\sin(2\pi(2f_s + f_r)t) \\ & + \frac{3}{2}\hat{I}_{E^{-}1}\hat{I}_{E^{+}1}\sin(2\pi(2f_r)t) + \frac{3}{2}\hat{I}_{TH1}\left(\hat{I}_{E^{-}1} - \hat{I}_{E^{+}1}\right)\sin(2\pi(f_r)t) \end{aligned} \tag{44}$$

Eq. (44) has a component at frequency $2f_s$, side-band components at $(2f_s \pm f_r)$ and

$2(f_s \pm f_r)$ and the additional components at f_r, $2f_r$,.Fig. 7 presents the spectrum of the PVPA and this harmonics with $f_r = f_s((1-s)/p)$ is a rotor frequency and p is a number of pole pairs.

We can deduce the expressions in a general way:

$$h = 1 \rightarrow 2f_s \tag{45}$$

With h is a pair number $h = 1, 3, 5, 7, \ldots$ it is more practical to take $TH = (h-1)f_s$

$h = 1 \rightarrow (2f_s + f_r)$ we can deduce a general formula $((h-1)f_r \pm kf_r)$ (46)

$h = 1 \rightarrow 2(f_s - f_r)$ we can deduce a general formula $(h-1)(f_s \pm kf_r)$ (47)

$h = 1 \rightarrow \begin{cases} f_r \\ 2f_r \end{cases}$ we can ,also ,deduce a general formula kf_r (48)

Therefore, we can draw that:

$TH = (h-1)f_s$ and $TH'' = kf$

$E^{\pm} = ((h-1)f_r \pm kf_r)$, $E^{\pm'} = (h-1)(f_s \pm kf_r)$

The amplitude of TH is more great that TH' because $\frac{3}{4}\hat{I}^2{}_{TH1} \rangle\rangle \frac{3}{2}\hat{I}_{E^+1}\hat{I}_{E^+1}$ and $\frac{3}{2}\hat{I}_{TH1}\left(\hat{I}_{E^+1} - \hat{I}_{E^+1}\right)$, In our comparison study case, we take only: $TH = (h-1)f_s$

The amplitude of $E^{\pm}$ is more great that $E^{\pm'}$ because $\frac{3}{2}\hat{I}_{TH1}\hat{I}_{E^+1} \rangle\rangle \frac{3}{4}\hat{I}^2{}_{E^+1}$ and $\frac{3}{2}\hat{I}_{TH1}\hat{I}_{E^-1} \rangle\rangle \frac{3}{4}\hat{I}^2{}_{E^-1}$

In our comparison study case, we take only: $((h-1)f_r \pm kf_r)$

From the same procedure for the other harmonics,

we do the same calculation, we find:

$$R^{\pm} = \left|\left((h-1)\pm 2ks\right)f_s\right|, R^{\pm'} = \left|\left(h\pm ks\right)f_s\right| \text{ and } \; R^{\pm''} = \left|\left(h\pm 2ks\right)f_s\right|$$
$$S^{\pm} = \left|\left((h-1)f_s \pm N_r(1-s)\right)f_s\right| \text{ and } \; S^{\pm'} = \left|hf_s \pm N_r\, f_r\right| \quad (49)$$

The same computations for a) and b) of Eq. (29).

It is noted that, our proposed approach HPVPA, PVSM , MSCSA and $PVSM_{P\text{-}H}$ has the same harmonics as those of PVPA cited, above. Without simplification of the computation, we find all the different harmonics in Table 2.

Note: Always, we will find the same expressions in the case where there would be a default, but we replace only $\hat{I}$ by $\hat{I}'$,with $\hat{I} \neq \hat{I}'$ and the same procedure for the following operations.

Table 2. General expression of the differrent harmonics for the other approaches studied

Harmonic Types	**The general expression of the HPVPA , PVPA , MSCSA, PVSM a) and $PVSM_{P\text{-}H}$ a) (The considered harmonics)**	**The general expression of the exclusive harmonics of the HPVPA , PVPA , MSCSA, PVSM and $PVSM_{P\text{-}H}$ (which are not considered in our study)**
Time Harmonics (TH):	$TH = (h-1)f_s$ a)	$TH' = hf_s$, $TH'' = kf_r$
Rotor Slot Harmonics (RSH)	$S^{\pm} = \left\|(h-1)f_s \pm N_r\, f_r\right\|$ a)	$S^{\pm} = \left\|hf_s \pm N_r\, f_r\right\|$
Rotor Bar Fault Harmonics (RBFH)	$R^{\pm} = \left\|\left((h-1)\pm 2ks\right)f_s\right\|$ a)	$R^{\pm'} = \left\|\left(h\pm ks\right)f_s\right\|, R^{\pm''} = \left\|\left(h\pm 2ks\right)f_s\right\|$
Eccentricity Fault Harmonics (EFH)	$E^{\pm} = \left\|(h-1)f_s \pm kf_r\right\|$ a)	$E^{\pm'} = \left\|(h-1)(f_s \pm kf_r)\right\|$

a) [8-10]

8. Experimental Results and Discussion

In this paper , the approaches studied above, were applied to a squirrel-cage induction motor under normal operation and Inter-turn short- circuits faults in the Stator Windings.The motor, used, in the Laboratory of Biskra university –Algeria -(Laboratoire de Génie Electrique de Biskra- LGEB-), is a three-phase squirrel-cage induction motor , 50 Hz, 3 kW, 4-poles

($p = 2$), Y connection , 200 turns per phase and with 28 rotor bars.

Normally, Fourier transform-based approaches are used for supervising power system harmonics. In order to maintain the computational accuracy of Fourier transform, the stationary and periodic characteristics of signals are generally required [30,31] .

Most references use a logarithmic Fast Fourier Transform FFT of the spectra benefiting from the effect of the logarithm, which raises the harmonics whose amplitudes are very low. .

Therefore, we will use an analysis logarithmic FFT of the spectra of the amplitudes for the studied approaches which can make the comparison between different methods of diagnosis.

Figs.3-7. clearly show the characteristic signatures of faulty stator, their amplitudes and their specific frequencies for all methods of diagnosis studied, above, depending on the motor state:

Case 1 - Motor is running under full load conditions: 100 % of its rated load $(s = 0.035)$.

a) – healthy motor.

b) – faulty stator: * Ntsc = 4 turns short-circuited (see Fig. 2).

* Ntsc = 10 turns short-circuited

Case 2 - Motor is running under medium load conditions : 60 % of its rated load $(s = 0.021)$.

a) – healthy motor.

b) – faulty stator: * Ntsc = 4 turns short-circuited .

* Ntsc = 10 turns short-circuited

Case 3 - Motor is running under low load conditions : 20 % of its rated load $(s = 0.0095)$.

a) – healthy motor.

b) – faulty stator: * Ntsc = 4 turns short-circuited.

* Ntsc = 10 turns short-circuited.

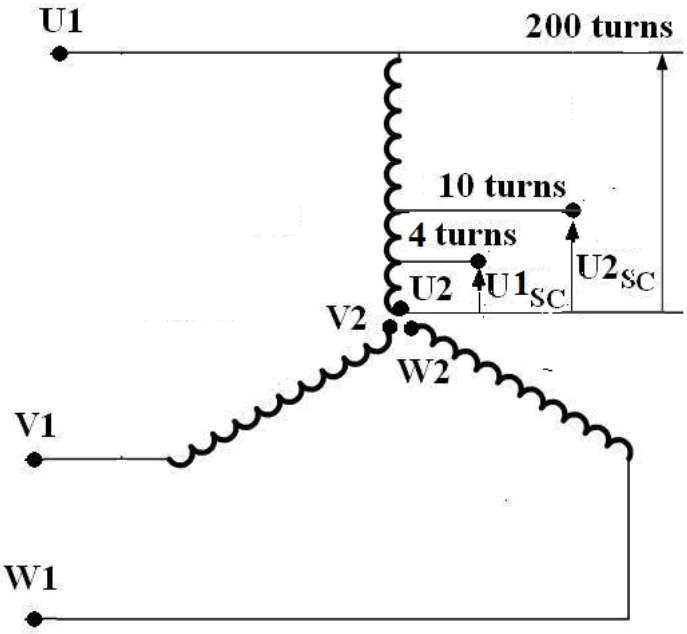

Fig. 2. Simplified representation showing how to make an inter-turn short- circuit in the stator windings

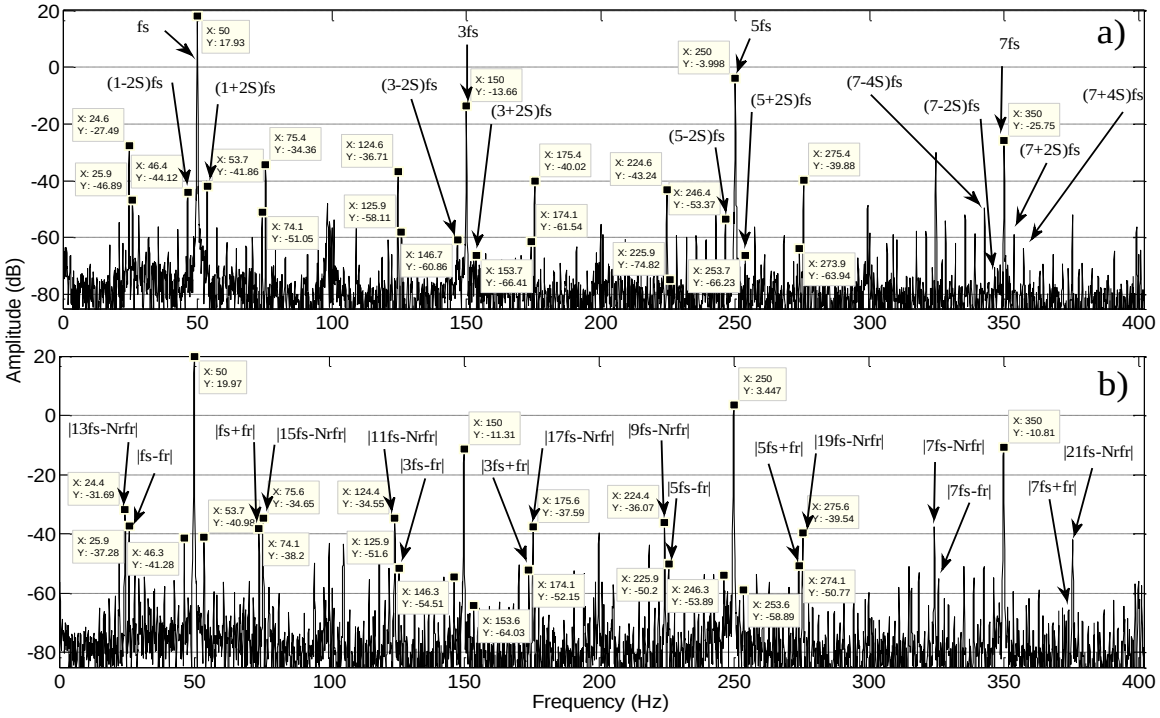

Fig. 3. Spectrum of the MCSA, for healthy motor (a) and with 10 turns short- circuited (b) (100 % of nominal load)

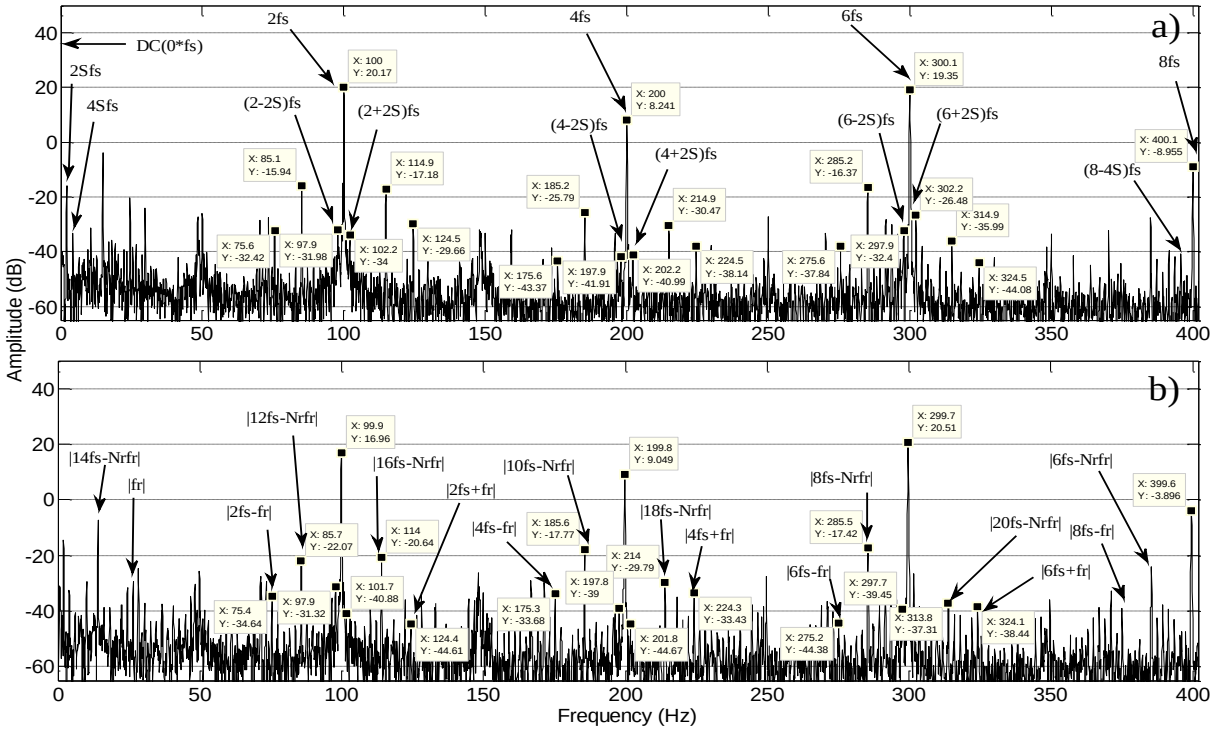

Fig.4. Spectrum of the PVSM, for healthy motor (a) and with 4 turns short- circuited (b) (60 % of nominal load)

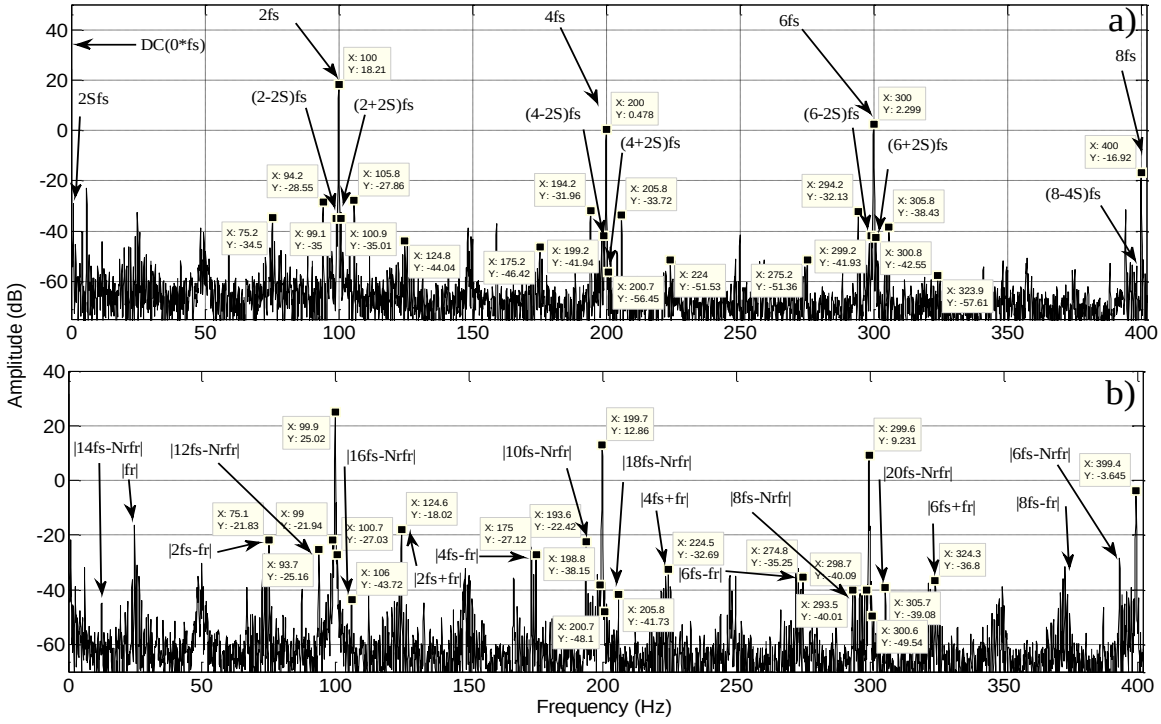

Fig.5. Spectrum of the MSCSA, for healthy motor (a) and with 10 turns short- circuited (b) (20 % of nominal load)

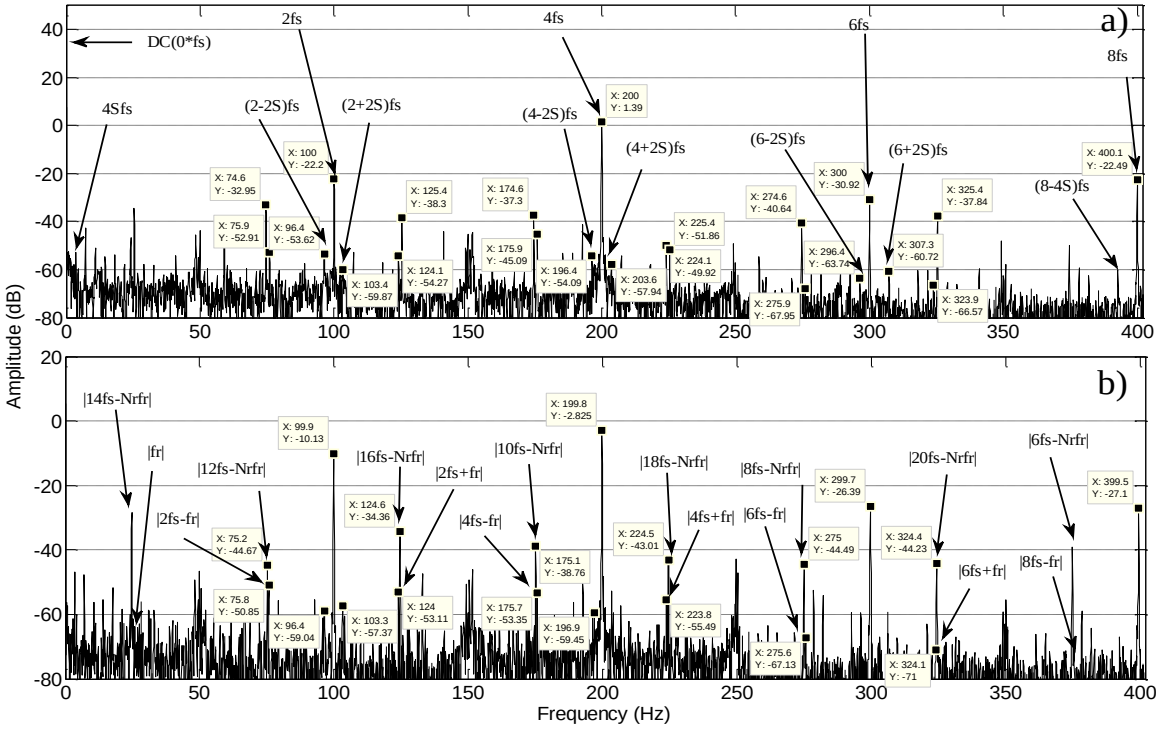

Fig. 6 Spectrum of the $PVSM_{P\text{-}H}$, for healthy motor (a) and with 4 turns short- circuited (b) (100 % of nominal load)

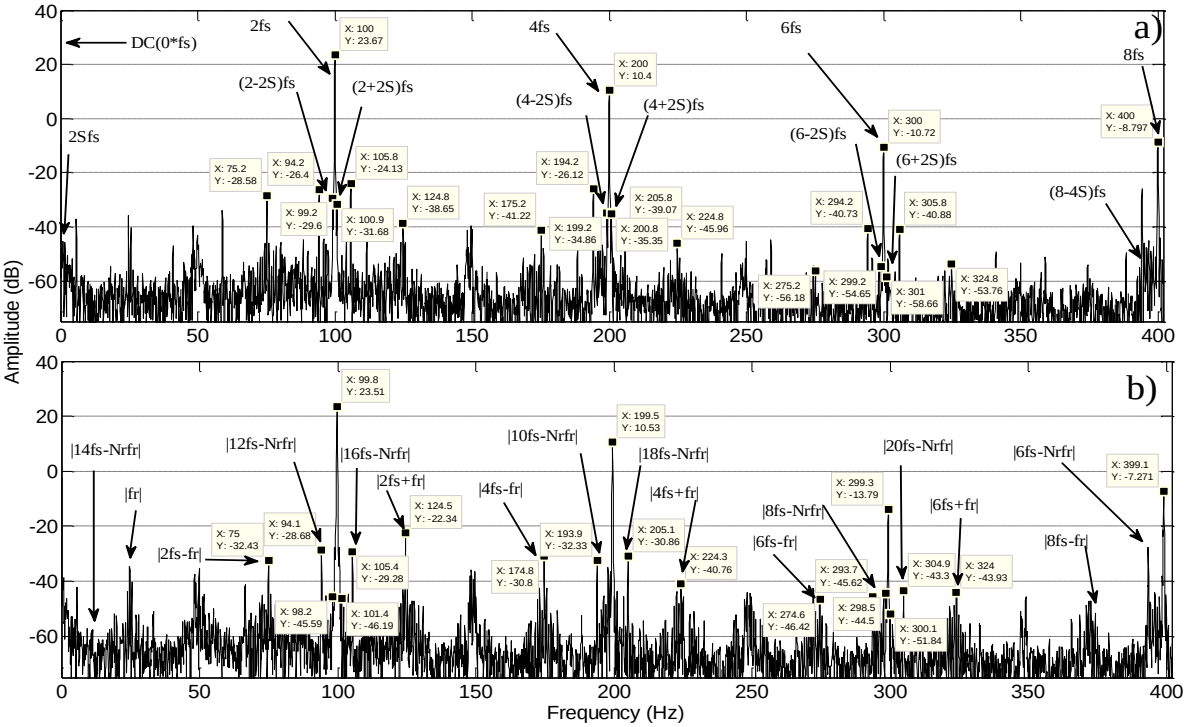

Fig. 7 Spectrum of the PVPA, for healthy motor (a) and with 4 turns short- circuited (b) (20 % of nominal load)

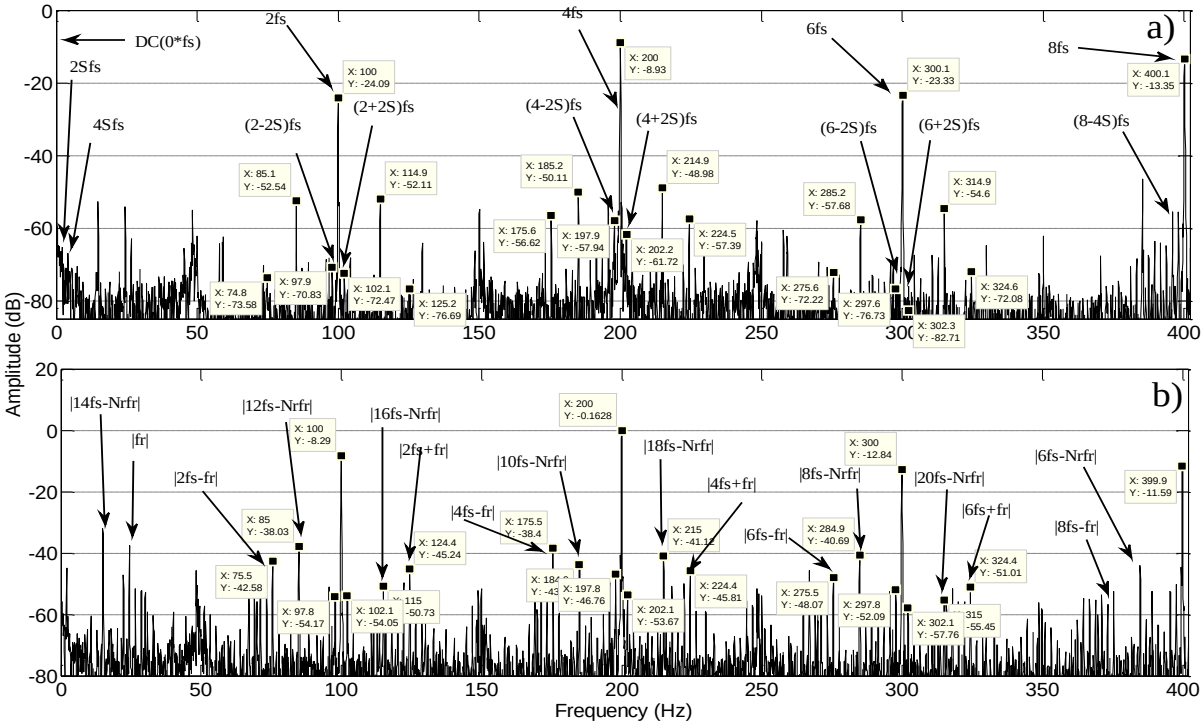

Fig. 8. Spectrum of the HPVPA , for healthy motor (a) and with 10 turns short- circuited (b) (60 % of nominal load)

To make a comparison of objective sensitivity between the six approaches in diagnosis. We must seek a very precise method recently used in specialized publications.

8.1. Comparative study using the Global Relative Indexes

The principle of this method is used by [8-9,18,32] , but we have improved it.This method improved has been used since it can give an excellent comparison between the different studied approache.This method improved gives us an overall result of all amplitudes differences between the healthy state and defaulting state. Therefore, we will use the "partial relative indexes " ($PRI_{AP.H}$)for all approaches and for each type of harmonic , according to eq.(50) ,Fig.9 and Fig.10:

Table 3. Cconsidered harmonics which are used to calculate $PRI_{AP.H}$

Harmonic Types	**Expressions of the considered harmonics MSCSA, PVSM, $PVSM_{P-H}$,PVPA, HPVPA**	**Expressions of the considered harmonics MCSA**
Time Harmonics (TH):	$-TH = (h-1)f_s$	$-TH = hf_s$
	with $h = 3,5,7,9.$	with $h = 1,3,5,7.$
Rotor Slot Harmonics (RSH)	$-S^{-} = \lvert(h-1)f_s - N_r f_r\rvert$	$-S^{-} = \lvert hf_s - N_r f_r\rvert$
	with $h = 9,11,13,17,19,21$	with $h = 9,11,13,15,17,19.$
Rotor Bar Fault Harmonics (RBFH)	$-R^{\pm} = \lvert((h-1)\pm 2s)f_s\rvert$	$-R^{\pm} = \lvert(h\pm 2s)f_s\rvert$
	with $h = 3,5,7.$	with $h = 1,3,5.$
Eccentricity Fault Harmonics (EFH)	$-E^{\pm} = \lvert(h-1)f_s \pm f_r\rvert$	$-E^{\pm} = \lvert hf_s \pm f_r\rvert$
	with $h = 3,5,7.$	with $h = 1,3,5.$

$AP = MCSA, PVSM, PVSM_{P-H}$ *or* $HPVPA$ and $H = TH, RSH, RBFH$ *or* EFH

$N_{AP.H}$: number of harmonics taken into consideration ($N_{AP.TH}$ = 4 and $N_{AP.RSH}$ = $N_{AP.RBFH}$ = $N_{AP.EFH}$ = 6).

We will change the reference point, by adding 120 dB, for rendering all data in positive number in order to simplify the computation depending on eq.(50).

Our analytical computation will extend to the frequency 400 Hz, taking into account the harmonics whose amplitudes are more important according to Table.3.

$$PRI_{AP.H} = \frac{\left(\frac{\sum_{i=1}^{N_{AP.H}} [Amplitude(AP.H)_i + 120]}{N_{AP.H}} \right)_{FaultyState}}{\left(\frac{\sum_{i=1}^{N_{AP.H}} [Amplitude(AP.H)_i + 120]}{N_{AP.H}} \right)_{HealthyState}} \quad (50)$$

We begin our calculation by the ideal motor operating mode: motor is running under full load (100 % of its rated load).

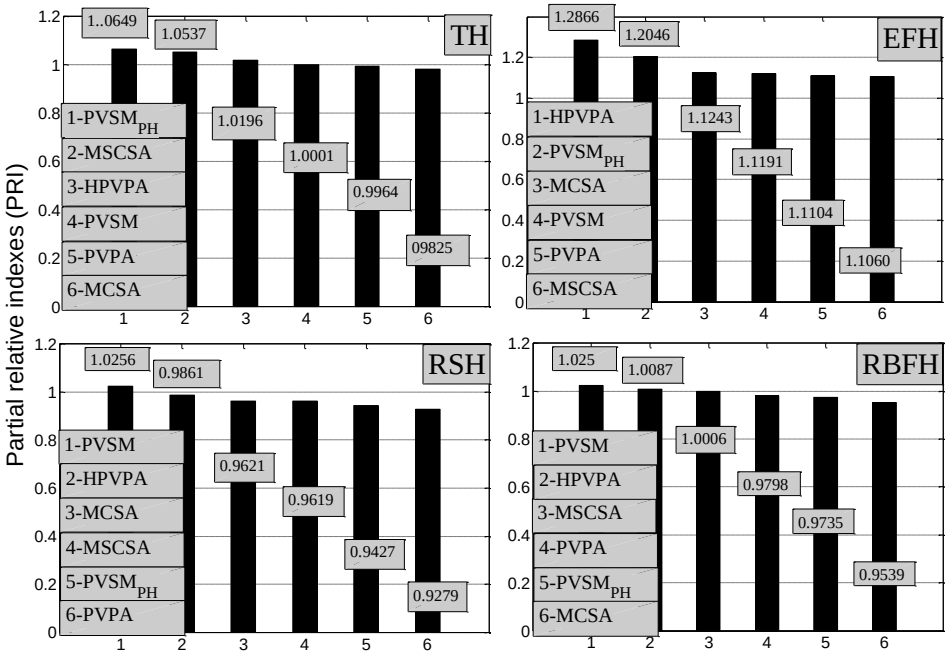

Fig. 9. Different partial relative indexes (PRI) corresponding to each approach with 4 turns short- circuited(20 % of nominal load)

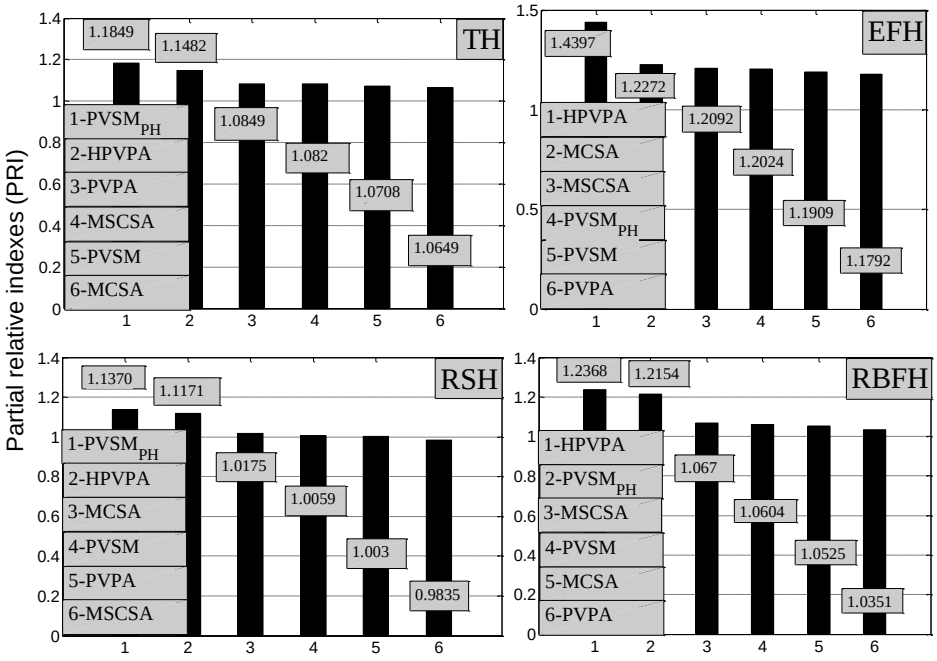

Fig. 10. Different partial relative indexes (PRI) corresponding to each approach with 10 turns short- circuited(100 % of nominal load)

Finally, we find the "global relative indexes "(GRI) that will give us a global sensitivity for each approach:

$$GRI_{AP} = \frac{PRI_{AP.TH} + PRI_{AP.RSH} + PRI_{AP.RBFH} + PRI_{AP.EFH}}{4} \quad (51)$$

Figures 11 and 12 give the ranking of different approaches depending on their sensitivity, by using global relative indexes method; it is clearly shown that the approach HPVPA has been classified in the first position under full load excepted in figure 11-d.

For the second case, motor is running under low load (20 % of its rated load), the same work is doing, while the third case under medium load (60 % of its rated load).

Figure 13 shows that HPVPA is more sensitive than all other diagnosis techniques for different regimes of motor operation with 4 and 10 turns into short- circuit in phase 1.

Thus, the final ranking of the sensitivity approaches, which we have studied, is given in figure 3 and table 4 with their most sensitive types of harmonics.

The proposed HPVPA approach has occupied the first sensitivity place for this type of fault.

This proves that this technique is highly sensitive than any other recent approaches found in the diagnostic literatures.

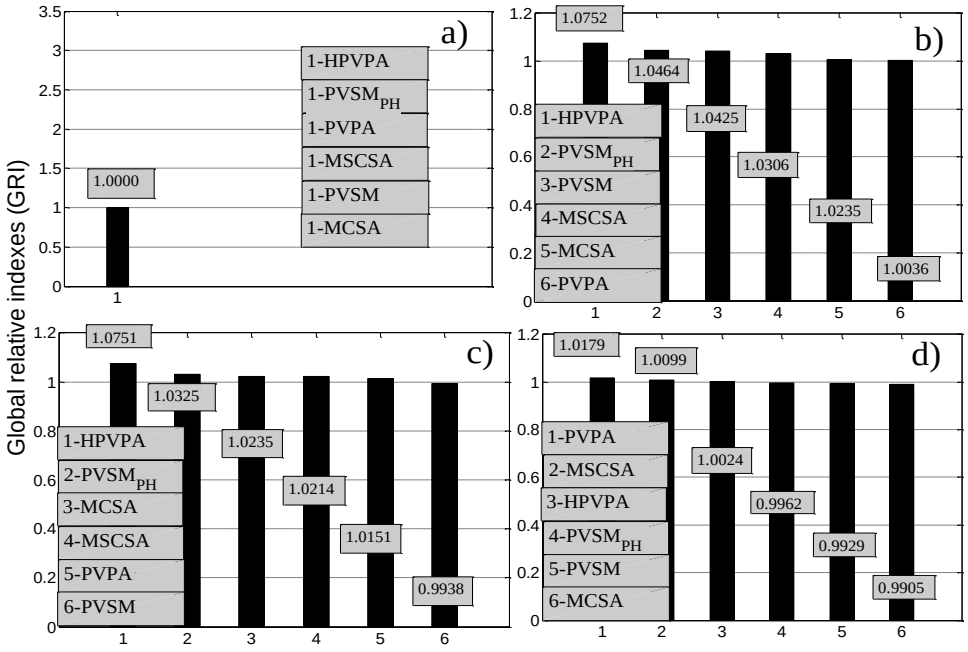

Fig.11. Different global relative indexes (GRI) corresponding to each approach for healthy state with various loads (a) and with 4 turns short-circuited under: low load (b) , medium load (c), and full load (d)

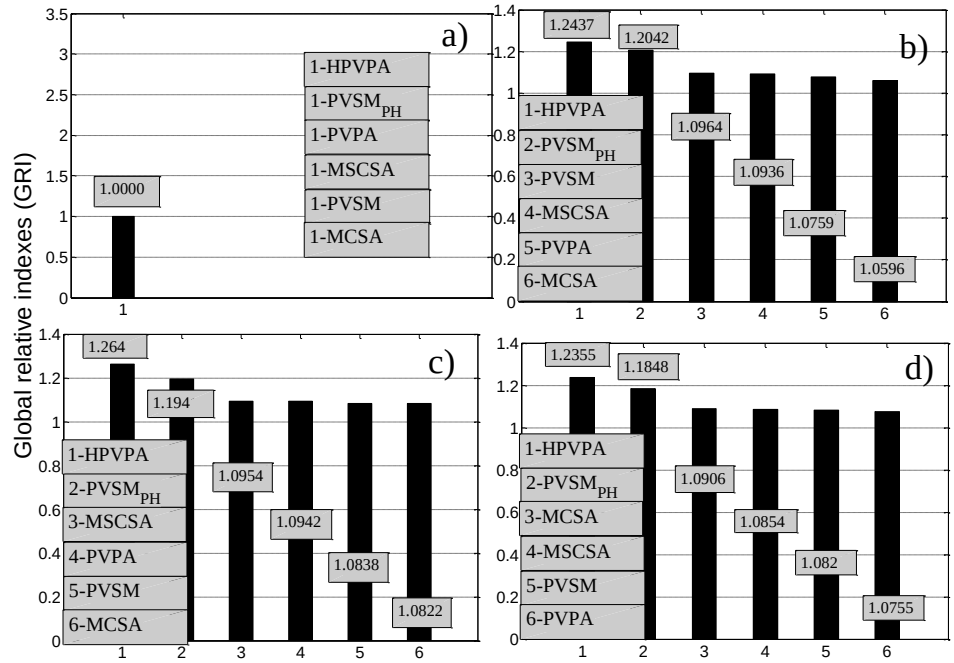

Fig.12. Different global relative indexes (GRI) corresponding to each approach for healthy state with various loads (a) and with 10 turns short-circuited under: low load (b) , medium

load (c), and full load (d).

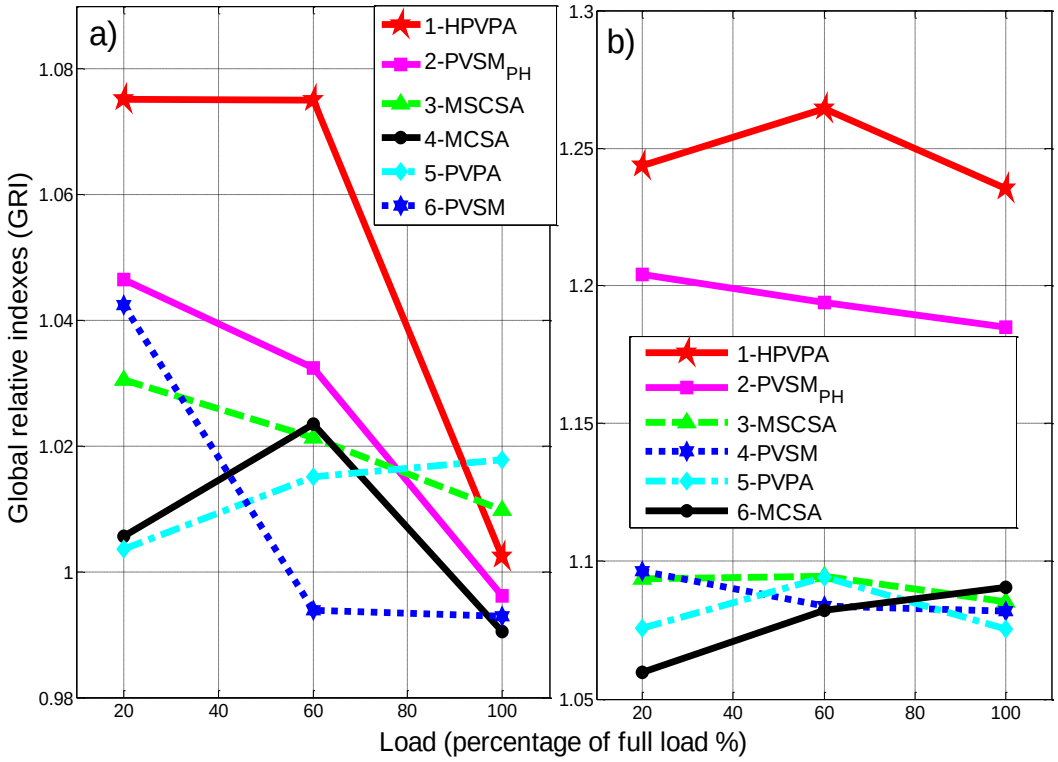

Fig.13. Experimental sensitivity of HPVPA proposed compared to other recent diagnosis techniques (with,4 turns into short-circuit a) and 10 turns into short-circuit b))

9. Conclusion

This study was based on an experimental test bench which extremely provided very accurate results .Thus; a comparison between the different approaches recently used in the field of diagnosis was well satisfied. These experimental results have lead to find a particular approach which really has a high sensitivity compared to the other recently published techniques.

According to Figs.3- 13, it is very rare to find an approach with a very high sensitivity comparable to these methods diagnosis recently published ,such as our proposed technique.

Finally, we have already laid hands on a unique method HPVPA whose sensitivity absolutely dominates all other modern techniques ,which have been classified, according to their sensitivity, successively PVSM$_{P\text{-}H}$, MSCSA, PVSM ,MCSA and PVPA and which covers broadly : the detection of Inter-turn short- circuits in induction motor (see Fig. 13). Especially, the surveys related to induction machine have reported that a large percentage of their defaults ,who is caused by stator winding faults .

This work is devoted to incipient faults detection of stator. This gives the possibility to move from preventive maintenance to predictive maintenance in aim to avoid unscheduled stops and ensuing costs, which assure a reliable chain of production.

References

1. M .Blodt, P. Granjon, B . Raison, et al.,models for bearing damage detection in induction motors using stator current monitoring, IEEE Trans. Ind. Electron.,Vol 55, (No. 4), 2008, p 1813- 1822. https://doi.org/10.1109/TIE.2008.917108
2. K. Holmberg, A . Adgar,A. Arnaiz , et al, (Eds.) .E-maintenance. London : Springer -Verlag 2010.
3. E. Lughofer, E. P. Klement,Model-based fault detection in multi-sensor measurement systems, Technical report Flll/Tr/0303, Johannes Kepler University Linz, Austria.
4. S. Ben Salem , K. Bacha , Chaari. A, Support vector machine-based decision for induction motor fault diagnosis using air-gap torque frequency response, International Journal of Computer Applications, Vol 38 (No.5),2012,p 27-33. DOI: 10.5120/4606-6812.
5. S. Ben Salem,K. Bacha , Chaari. A ,Support vector machine based decision for mechanical fault condition monitoring in induction motor using an advanced Hilbert-Park transform ,ISA Trans., Vol 51(No.5),2012, p 566–572. https://doi.org/10.1016/j.isatra.2012.06.002
6. T. Sribovornmongkol ,Evaluation of motor online diagnosis by FEM simulations, Master's Thesis ,Royal Institute of Technology Stockholm, Sweden , 2006.
7. K. Bacha, S. Ben Salem, A. Chaari , An improved combination of Hilbert and Park transforms for fault detection and identification in three-phase induction motors , Electrical Power and Energy Systems ,Vol 43 (No.1),2012, p1006–1016. https://doi.org/10.1016/j.ijepes.2012.06.056

8. M. Sahraoui , A. Ghoggal, S. Guedidi , et al. ,Detection of inter-turn short-circuit in induction motors using Park–Hilbert method, International Journal of System Assurance Engineering and Management , Vol 5 (No.3),2014,p 337-351. DOI: 10.1007/s13198-013-0173-6
9. M. Sahraoui , Etude comparative des méthodes de diagnostic des machines asynchrones (Comparative study of the methods of diagnosis in the asynchronous machines), Thesis for the degree of Doctor of Science, Biskra university ,Algeria, 2010.(in French).
10. M. Sahraoui , S. E. Zouzou, A. Ghoggal ,et al. ,A new method to detect inter-turn short- circuit in induction motors,19nd ed., International conference on Electrical Machine (ICEM,2010), Sept ,2010,(Rome,Italy), IEEE, 2010 ,p 1-6. https://doi.org/10.1109/ICELMACH.2010.5607854
11. V. F. Pires, M. Kadivonga , J. F. Martins ,et al. ,Motor square current signature analysis for induction motor rotor diagnosis , Measurement , Vol 46 (No.2), 2013, p 942–948. https://doi.org/10.1016/j.measurement.2012.10.
12. I. Aydin, M. Karakose, E. Akin ,A new method for early fault detection and diagnosis of broken rotor bars, Energy Conversion and Management, Vol 52 (No.4) , 2011, P 1790–1799 https://doi.org/10.1016/j.enconman.2010.11.018
13. A. Allal, B. Chetate , A new and best approach for early detection of rotor and stator faults in induction motors coupled to variable loads,Frontiers in Energy, Vol 10 (No.2),2016, P 176-191.DOI: 10.1007/s11708-015-0386-2
14. A. Allal, Nouvelles méthodes et techniques de diagnostic des machines asynchrones à rotor en cage d'écureuil (New methods and diagnostic techniques asynchronous machines of squirrel cage rotor)), Thesis for the degree of Doctor of Science, Boumerdes university, Algeria, 2017.(in French).

15. M. Boucherma, M. Y. Kaikaa ,A. Khezzar , Park model of squirrel cage induction machine including space harmonics effect, Journal of Electrical Engineering , Vo l 57 (No.4), 2006, p 193-199 .
16. J. Huppunen ,High-speed solid-rotor induction machine electromagnetic calculation and desing,Thesis for the degree of Doctor of Science, Lappeenranta University of Technology, Finland, 2004.
17. G. Joksimović, J. Riger , T. Wolbank , et al.,Stator line current spectrum content of a healthy cage rotor induction machine, In Diagnostics for Electric Machines, Power Electronics & Drives (SDEMPED), IEEE International Symposium on. Sept, IEEE , 2011,p 113-118. https://doi.org/10.1109/DEMPED.2011.6063610
18. S. E. Zouzou. , M. Sahraoui, A. Ghoggal, et al. ,Detection of inter- turn short-circuit and broken rotor bars in induction motors using the partial relative indexes: application on the MCSA, 19nd ed., International conference on Electrical Machine (ICEM,2010), Sept ,2010,(Rome,Italy), IEEE, 2010 ,p 1-6. https://doi.org/10.1109/ICELMACH.2010.5607874
19. R. Kechida, A. Menacer, , H. Talhaoui , Approach signal for rotor fault detection in induction Motors,Journal of failure analysis and prevention, Vol 13 (No.3), 2013,p 346-352.
20. G. Didier, E. Ternisien, O. Caspary, et al. , A new approach to detect broken rotor bars in induction machines by current spectrum analysis, Mechanical Systems and Signal Processing,Vol 21(No.2), 2007, p 1127-1142. https://doi.org/10.1016/j.ymssp.2006.03.002
21. M. U. Petushkov, Analysis of defects in the rotor asynchronous motor during star, International Journal of applied and fundamental research , (No.1), 2013, p 1-1.
22. A. Allal , Grandeurs non invasives pour le diagnostic des machines asynchrones (Non-Invasive Quantities for Diagnosis of Asynchronous Machines), Thesis for the degree of Magister , University of Sétif, Algeria, 2010.(in French).
23. A. B. Amar ,Direct Torque Control of a Doubly Fed Induction Generator, International Journal of Energetica, Vol 2 (No.1), 2017 ,p 11-14.
24. J. Zarei , J. Poshtan , An advanced Park's vectors approach for bearing fault detection, Tribol. Int., Vol 42(No.2), 2009, p 213-219. https://doi.org/10.1016/j.triboint.2008.06.002

25. A. Kumar ,A new method for early detection of inter-turn shorts in induction motors , 2nd International Conference on Power and Energy Systems ,2012 , (Singapore), IACSIT Press,2012, vol. 56, p. 41..
26. A. Djebala,N. Ouelaa , C. Benchaabane , et al. , Application of the wavelet multi-resolution analysis and Hilbert transform for the prediction of gear tooth defects, Meccanica, Springer Netherlands, Vol 47 (No.7), 2012, p 1601-1612. DOI: 10.1007/s11012-012-9538-1
27. S. K. Ahamed , M. Mitra , S. Sengupta ,et al., Identification of mass-unbalance in rotor of an induction motor through envelope analysis of motor starting current at no load, Journal of Engineering Science and Technology Review , Vol 5 (No.1), 2012 ,p 83-89 .
28. A. Allal , B. Chetate , D. Benattous ,The Instantaneous Power Approach for Rotor Cage Fault Diagnosis in Induction Motor**,** 6 th symposium on Hydrocarbons and chemistry ISHC6,2012,(Zeralda , Algiers) .
29. Z. Glowacz, J. Kozik , Detection of synchronous motor inter-tern faults based on spectral analysis of Park's vector, Arch. Metall. Mater., Vol 58 (No.1), 2013 ,p 19-23. https://doi.org/10.2478/v10172-012-0144-y
30. L. Qi , S. Woodruff , L. Qian , et al. , Eds.Prony analysis for time – Varying harmonics,Time-Varying Waveform Distortions in Power Systems, Edited by Paulo Fernando Ribeiro, JohnWiley & Sons, 2009..
31. J. Cusidó, L. Romeral , J. A. Ortega , et al. ,Signal Injections as a Fault Detection Technique, Sensors Vol 11(No.3), 2011, p 3356-3380. http://dx.doi.org/10.3390/s110303356
32. G. Didier, E. Ternisien ,O. Caspary, et al., Fault detection of broken rotor bars in induction motor using a global fault index, IEEE Trans. Ind. Appl., Vol 42 (No.1), 2006 ,p 79-88.

How to cite this article:
Allal A and Chetate B. High sensitivity detection of the stator short-circuit faults in induction motor using Hilbert Park's vector product. J. Fundam. Appl. Sci., 2019, *11(2), 994-1022.*